Journal of the Serbian Chemical Society
JSCS-info@shd.org.rs • www.shd.org.rs/JSCS
J. Serb. Chem. Soc. 76 (12) 1673–1685 (2011)
JSCS–4239
UDC 542.913–732:546.92'97'811–44:547.262+66.094.3
Original scientific paper

Microwave synthesis and characterization of Pt and Pt–Rh–Sn electrocatalysts for ethanol oxidation

SANJA STEVANOVIĆ[1*#], DUŠAN TRIPKOVIĆ[2#], DEJAN POLETI[3#], JELENA ROGAN[3#], AMALIJA TRIPKOVIĆ[1#] and VLADISLAVA M. JOVANOVIĆ[1]

[1]*Department of Electrochemistry, ICTM, University of Belgrade, Njegoševa 12, Belgrade, Serbia,* [2]*Materials Science Division, Argonne National Laboratory, Argonne, IL 60439, USA and* [3]*Faculty of Technology and Metallurgy, University of Belgrade, Karnegijeva 4, Belgrade, Serbia*

(Received 5, revised 29 April 2011)

Abstract: Carbon-supported Pt and Pt–Rh–Sn catalysts were synthesized by the microwave-polyol method in ethylene glycol solution and were investigated in the ethanol electro-oxidation reaction. The catalysts were characterized in terms of structure, morphology and composition employing the X-ray diffraction (XRD), scanning tunneling microscopy and energy-dispersive X-ray spectroscopy techniques. The STM analysis indicated rather uniform particles and particle sizes below 2 nm for both catalysts. The XRD analysis of the Pt/C catalyst revealed two phases, one with the main characteristic peaks of the face-centered cubic crystal structure (*fcc*) of platinum and the other related to the graphite-like structure of the carbon support, Vulcan XC-72R. However, in the XRD pattern of the Pt–Rh–Sn/C catalyst, diffraction peaks for Pt, Rh or Sn could not be resolved, indicating extremely low crystallinity. The small particle sizes and homogeneous size distributions of both catalysts could be attributed to the advantages of the microwave-assisted modified polyol process in ethylene glycol solution. The Pt–Rh–Sn/C catalyst was highly active for ethanol oxidation with the onset potential shifted by more than 150 mV to more negative values and with currents nearly 5 times higher in comparison to the Pt/C catalyst. The stability tests of the catalysts, as studied by chronoamperometric experiments, revealed that the Pt–Rh–Sn/C catalyst was evidently less poisoned than the Pt/C catalyst. The increased activity of Pt–Rh–Sn/C in comparison to Pt/C catalyst was most probably promoted by the bi-functional mechanism and the electronic effect of the alloyed metals.

Keywords: Pt–Rh–Sn catalyst; ethanol oxidation; polyol synthesis; microwave irradiation; STM.

* Corresponding author. E-mail: sanjat@tmf.bg.ac.rs
# Serbian Chemical Society member.
doi: 10.2298/JSC110405166S

INTRODUCTION

High surface area carbon-supported Pt and Pt-alloys are widely proposed as promising anode catalysts in direct alcohol fuel cells (DAFCs).[1] Platinum is an excellent catalyst for the adsorption and dissociation of small organic molecules. However, platinum itself is known to be rapidly poisoned by reaction intermediates, such as CO, that are formed by dehydrogenation of the alcohol molecule[2] and limited ability for cleavage of C−C bonds. The most common fuel besides methanol is ethanol, which is less toxic and can be easily produced by fermentation of sugar-containing biomass. The oxidation mechanism of ethanol in acid solution may be summarized in the following schema of parallel reactions:[1]

$$CH_3CH_2OH \rightarrow [CH_3CH_2OH]_{ad} \rightarrow C1_{ad}, C2_{ad} \rightarrow CO_2 \text{ (total oxidation)} \quad (1)$$

$$CH_3CH_2OH \rightarrow [CH_3CH_2OH]_{ad} \rightarrow CH_3CHO \rightarrow CH_3COOH \text{ (partial oxidation)} \quad (2)$$

Differential mass spectrometry (DEMS) and *in situ* infrared spectroscopy (FTIR) determined acetaldehyde (CH_3CHO) and acetic acid (CH_3COOH) as the main products of the oxidation of ethanol in acidic solution, with carbon dioxide (CO_2) appearing at very high positive potentials.[3,4] The efficiency of C−C bond cleavage is the key to enable this reaction to be useful in fuel cell applications and thus, the major challenge is to achieve total oxidation of ethanol to CO_2 at low overpotentials. Efforts in this sense have been focused on the addition of co-catalysts, such as Ru, Rh, W, Pd, Sn, *etc*.[1,5–10] The addition of metals such as Sn or Ru, even though beneficial for the overall electrochemical activity of the catalysts for ethanol oxidation, does not enhance the yield of CO_2, *i.e*., C−C bond breakage.[4,11] On the other hand, the addition of Rh to Pt improves the activation for C−C bond dissociation, but does not enhance the overall electrochemical reaction.[9,10] Thus, a good electrocatalyst for ethanol oxidation should have, besides Pt, both kind of metals that would improve dehydrogenation, C−C bond dissociation and CO–O coupling.[9] Different ternary catalysts have been described in the literature[1] (and references therein), but although PtSn appears to enhance ethanol oxidation better than other bimetallic catalysts and presence of Rh significantly increases C−C bond breakage, there are only a few data on ternary Pt catalyst with Sn and Rh.[12–14] Colmati *et al*.[12] investigated the activity for ethanol oxidation of Pt–Rh–Sn catalysts and found that at potentials higher than 0.45 V *vs*. RHE, the alloy possessed the highest activity for this reaction, while at potentials more negative than 0.45 V, the activity was lower than that of the binary PtSn catalyst. Kowal *et al*.[13] indicated that Pt–Rh–SnO_2 exhibited higher activity than $PtSnO_2$ even at lower potentials. The extent of activity of such catalyst depends strongly on the SnO_2 content.[14]

In general, metal catalytic activity is considerably dependent on the particle shape, size and particle size distribution.[15] A variety of methods can be used for nanocatalyst preparation, such as wet impregnation, sonochemical method, che-

mical reduction of metal precursors, *etc*. In the last decade, Pt or Pt-based nanoclusters with small particle size and narrow size distribution have often been synthesized by the polyol method.[16] This procedure, as most of the other conventional methods, requires longer treatment of metal precursors at a high temperature. To overcome the arduous processes, in recent years, microwave irradiation has been widely used for the preparation of nanomaterials. Compared with conventional preparation methods, microwave synthesis has the advantages of very short heating time and uniform heating of the substance, leading to a small particle size, narrow particle size distribution and high purity. Yu *et al*.[17] suggested that these advantages could be attributed to fast homogenous nucleation and growth of metal particles.

The goal of this work was to examine ethanol oxidation on a carbon-supported Pt–Rh–Sn catalyst synthesized by the microwave-assisted polyol method. This procedure for the preparation of the previously mentioned catalyst, to the best of our knowledge, has not hitherto been described in the literature.

EXPERIMENTAL

Preparation of Pt and Pt–Rh–Sn/C electocatalysts

To prepare Pt–Rh–Sn catalyst, a mixture of 0.5 ml of 0.05 M H_2PtCl_6, 0.5 ml of 0.1 M $SnCl_2$ solution and 0.5 ml 0.05M of $RhCl_3$ was mixed with 25 ml of ethylene glycol (EG) in a 100 ml beaker under magnetic stirring. Then 0.8 M NaOH was added drop wise to adjust the pH to ≈12. The same procedure was used to synthesize the Pt catalyst. In each case, the beaker was placed in the center of a domestic microwave oven and heated 60 s for the Pt and 90 s for Pt–Rh–Sn catalyst at 700 W. After microwave heating, the mixture was uniformly mixed with 20 ml of an aqueous suspension of Vulcan XC-72 carbon (containing 20 mg of carbon in the case of Pt catalyst and 53.5 mg of carbon in the case of Pt–Rh–Sn catalyst) and 150 ml of 2 M H_2SO_4 solution for 3 h under magnetic stirring. The resulting suspension was filtered and the residue was washed with high purity water. The solid product was dried at 160 °C for 3 h under a N_2 atmosphere. The metal loading for both catalysts should have been ≈20 wt. %. Thermogravimetric analysis (TGA) confirmed 19 wt. % for Pt/C, while for Pt–Rh–Sn/C, a lower loading of metal (≈11 wt. %) was found.

Characterization of the Pt/C and Pt–Rh–Sn/C electrocatalysts

Thermogravimetry (TG) and differential thermal analyses (DTA) were performed simultaneously (30–800 °C temperature range) on a SDT Q600 TGA/DSC instrument (TA Instruments). The heating rate was 20 °C min^{-1} and the sample mass was less than 10 mg. The furnace atmosphere consisted of air at a flow rate of 100 cm^3 min^{-1}.

The unsupported Pt and Pt–Rh–Sn nanoparticles were characterized by scanning tunneling microscopy (STM). Samples were prepared by applying a few drops of a diluted colloidal solution of catalyst on a hot HOPG plate. The STM characterizations were realized using a NanoScope III A (Veeco, USA) microscope. The images were obtained in the height mode using a Pt–Ir tip (set-point current, I_t, from 1 to 2 nA, bias voltage, V_b = –300 mV). The mean particle size and size distribution were acquired from several randomly chosen areas of the STM images containing about 50 particles.

X-Ray diffraction (XRD) patterns of the powder catalysts were recorded with an Ital Structure APD2000 X-ray diffractometer in Bragg–Brentano geometry using CuK_α radiation (λ = 0.15418 nm) in the step-scan mode (range: 15−85° 2θ, step-time: 2.50 s, step-width: 0.02°). The program PowderCell [18] was used for phase analysis and calculation of the unit cell parameters.

Microstructural examination was performed by scanning electron microscopy (SEM). An XL 30 environmental scanning microscope with a field emission gun (ESEM–FEG) (manufactured by FEI, The Netherlands) equipped with an energy dispersive X-ray (EDX) spectrometer was used. The samples were inspected using 5, 10 and 20 kV acceleration voltages at magnifications of 20000× and 10000×.

The electrocatalytic activity of the catalysts was investigated by potentiodynamic and chronoamperometric tests using an Autolab potentiostat/galvanostat (ECO Chemie, The Netherlands) and a three-electrode compartment cell at room temperature. The working electrode was a thin layer of Nafion-impregnated Pt/C or Pt–Rh–Sn/C catalyst applied on a glassy carbon disk electrode with a loading of 10 μg cm^{-2} of the catalyst counted on metal content. The thin layer was obtained from a suspension of 2 mg of the Pt–Rh–Sn/C or 1 mg of Pt/C catalyst in a mixture of 1 ml water and 50 μl of 5 % aqueous Nafion solution, prepared in an ultrasonic bath, placed onto the substrate and dried at room temperature. A Pt wire and a saturated calomel electrode (SCE) were used as the counter and reference electrode, respectively. The electrocatalytic activity of the as-prepared Pt/C and Pt–Rh–Sn/C was studied in 0.1 M $HClO_4$ + 0.5 M C_2H_5OH solution. The electrolyte was prepared with high purity water and deaerated with N_2. Ethanol was added to the supporting electrolyte solution while holding the electrode potential at –0.2 V. The potential was then cycled up to 0.3 V, *i.e.*, the potential range of technical interest (E < 0.4 V), at sweep rate of 20 mV s^{-1}. Current–time transient curves were recorded after immersion of the freshly prepared electrode in the solution at –0.2 V for 2 s followed by stepping the potential to 0.2 V and holding the electrode at this potential for 30 min.

RESULTS AND DISCUSSION

Catalysts characterizations

The particle size and surface morphology of the unsupported Pt and Pt–Rh–Sn catalysts were characterized by STM. As observed from the top view of the STM images (Fig. 1), both catalysts had rather uniform particles of small diameter. Most of particles were spherical in shape. Cross section analysis (Fig. 1) confirmed particle sizes of < 1.7 nm for both catalysts (Table I).

The Pt/C and Pt–Rh–Sn/C catalysts were characterized by X-ray powder diffraction analysis. The XRD patterns of the carbon-supported catalysts are shown in Fig. 2. Two phases were identified in the Pt/C pattern, one with the main characteristic peaks of the face-centered cubic crystal structure (*fcc*) of platinum (111, 200, 220 and 311) and the other with a diffraction peak at around 2θ 25° related to the graphite-like structure of the Vulcan XC-72R carbon support. The XRD peaks of the Pt–Rh–Sn/C catalyst were rather broad and diffraction peaks for Pt, Rh and Sn in the catalyst could not be separately resolved, indicating a small metal content and a very low crystallinity or an amorphous form of the catalyst. Since TGA analysis revealed the presence of only 11 wt. % of the metals

in the supported catalyst and the STM analysis showed very small particle size, the low metal fraction and low crystallinity could be the reason for the obtained XRD pattern of the Pt–Rh–Sn/C catalyst. The mean particle size for the Pt/C catalyst calculated by the Scherrer formula[19] was larger than that obtained by STM (Table I), possibly because unsupported catalysts were used for the STM analysis. Still, the agreement can be described as good because the values calculated by the Scherrer formula also account for a very probable lattice stress.

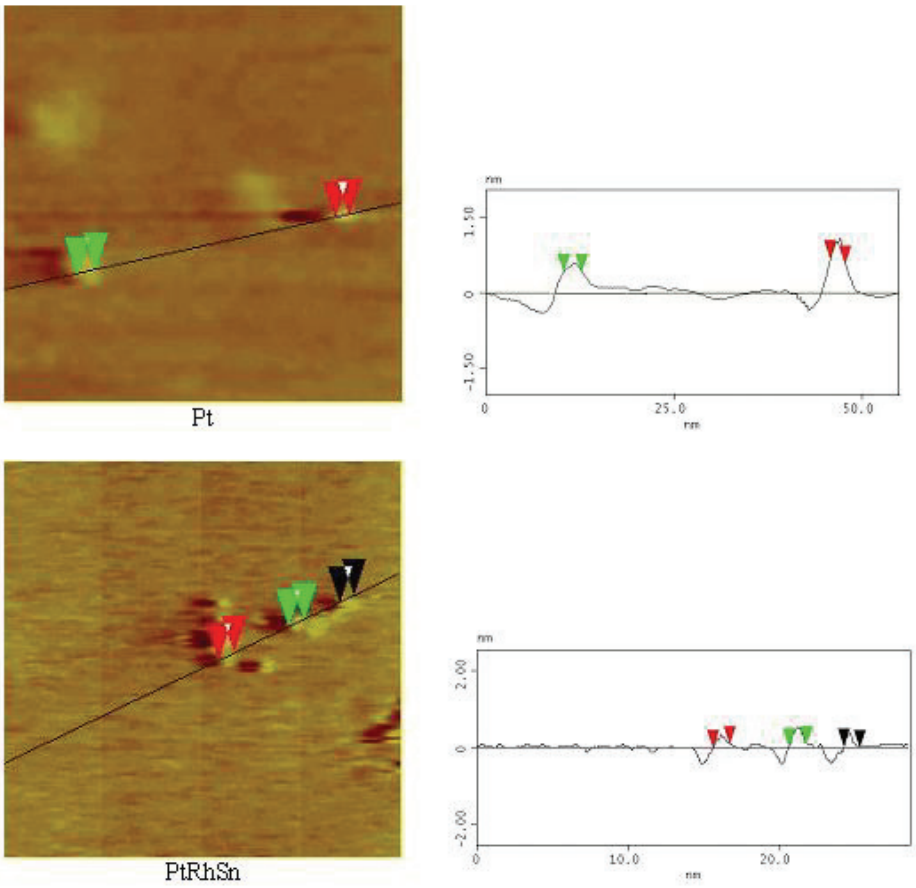

Fig. 1. STM Images and height profiles of the Pt catalyst (50×50 nm^2×4 nm) and Pt–Rh–Sn catalyst (30×30 nm^2×4 nm).

The small particle sizes and homogeneous size distributions of both catalysts could be attributed to the advantages of the microwave-assisted modified polyol process in which ethylene glycol (EG) and hydroxide are used as stabilizers. The metal salts and hydroxide react to form colloidal metal hydroxide particles, which are reduced to metal nanoclusters by EG.[16] In this process, pH value of the

TABLE I. Characteristics of the Pt/C and Pt–Rh–Sn/C catalysts obtained by STM, XRD and EDX analysis

Catalyst	Particle size, nm		Unit cell parameter (XRD), a / nm	Elemental composition (Pt:Rh:Sn), at. %	
	STM	XRD		Nominal	EDX
Pt/C	1.7±0.3	2.5	0.3944		
Pt–Rh–Sn/C	1.2±0.3	–	–	25:25:50	46:32:22

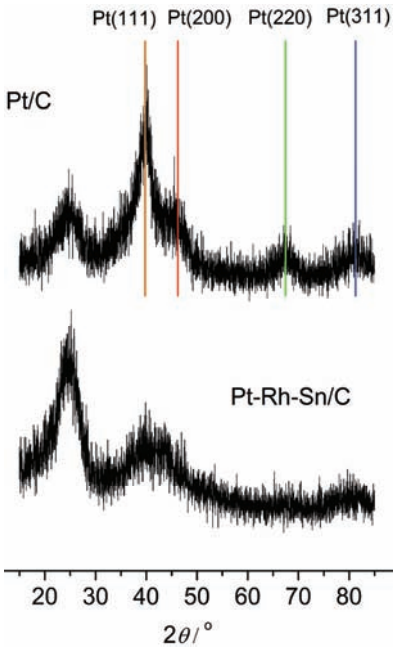

Fig. 2. XRD Patterns of the Pt /C and Pt–Rh–Sn/C catalysts.

solution is very important for obtaining stable metal particles. Hydroxide/metal molar ratio depends on the metal in question and is characteristic of electrostatic stabilization of metal colloids by the adsorbed anions.[16] EG acting as both reaction and dispersion media can efficiently adsorb and stabilize the surface of the particles[20] and favor the production of monodispersed metal particles with good dispersivity.[17] The high viscosity of this compound also helps in preventing agglomeration of the nanoparticles and for this reason, the water content in the reaction solution effects this process as well as the reaction temperature in influencing the particle size and size distribution.[21] Since EG has a large permanent dipole, it is very susceptible to microwave irradiation, which can absorb the energy from the microwave field and the polar reaction solution is heated up to a high temperature instantaneously.[22] Nevertheless, the heating rate of EG dispersion system could be affected by parameters of microwave operation, such as irradiation time, amount of dielectric and additives.[23] The fast and uniform microwave heating reduces the temperature and concentration gradients, thus accele-

rating the reduction of the metal ions and the formation of metallic nuclei.[24–27] In processes with plurality of pathways and activation barriers, according to Rao *et al*.[26], microwaves might promote the pathway with the lowest activation barrier.

EDX Analysis of the Pt–Rh–Sn/C surface composition gave 48 at. % Pt and 32 at. % Rh and 20 at. % Sn for the Pt–Rh–Sn alloy (Table I), which deviates from the nominal composition in the initial mixture (25:25:50).

Bearing in mind the aforesaid, the irradiation time in the microwave heating together with NaOH/metal and EG/water ratios used in the synthesis of both catalyst were probably the reason for the so small particle size obtained, and also for the yield of the metal and the catalyst composition.

Electrochemical performances

Ethanol oxidation was studied at the as-prepared Pt/C and Pt–Rh–Sn/C catalysts. The cyclic voltammogram for Pt–Rh–Sn/C after only two cycles to characterize roughly the surface but to avoid significant dissolution of Rh and Sn is shown in Fig. 3. The cyclic voltammograms for Pt/C are given as steady state and after two cycles for comparison. The steady state CV for Pt/C was similar to those for polycrystalline platinum or other Pt catalysts supported on high surface area carbon, with a well-defined region of hydrogen adsorption/desorption, separated by a double layer from the region of surface oxide formation. These regions were not well-defined at the beginning of cycling since the surface was still not fully reconstructed. The CV for Pt–Rh–Sn/C was similar to the CV for PtRh/C[10]

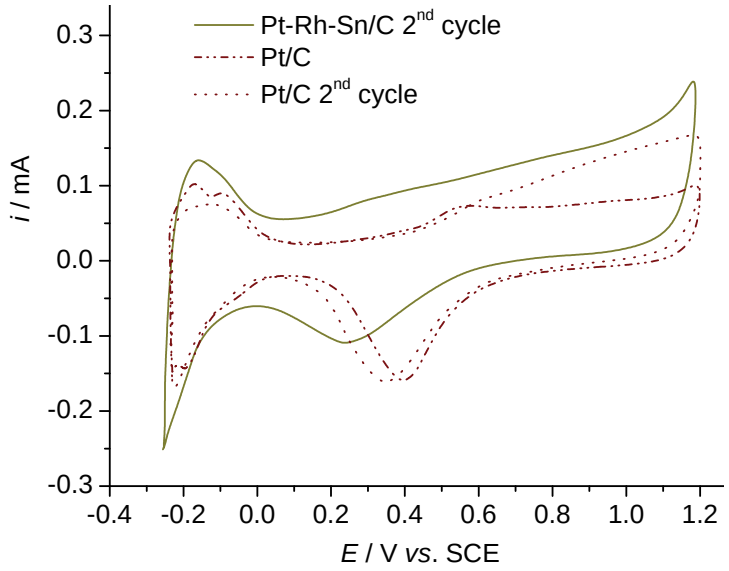

Fig. 3. Basic voltammograms of the Pt/C and Pt–Rh–Sn/C catalysts in 0.1 M $HClO_4$, v = 50 mV s^{-1}.

and is characterized by a large single peak in the hydrogen adsorption/desorption region, which Lima *et al.*[10] associated with adsorption/desorption of hydrogen on the intermetallic phase of PtRh. The shift of the reduction peak for Pt–Rh–Sn/C to more a negative potential value in comparison to Pt/C could be an indication of alloyed Pt and Rh. The larger double layer in the case of Pt–Rh–Sn/C compared to Pt/C was due to the lower metal content (11 mass %) of this catalyst in comparison to Pt/C (20 mass %).

The electrocatalytic activities of the as-prepared catalysts were studied in 0.1 M $HClO_4$ + 0.5 M C_2H_5OH solution and the positive scan voltammetric curves are presented in Fig. 4. The Pt–Rh–Sn/C catalyst was highly active in ethanol oxidation with the onset potential at approximately –0.15 V (shifted by ≈0.15 V towards more negative potentials compared to Pt/C) and rapid kinetics. The hydrogen adsorption/desorption peaks were clearly suppressed because the ethanol adsorption displaced the adsorbed hydrogen from the interface. The current densities, calculated on Pt content, throughout the studied potential region were five times higher for the Pt–Rh–Sn/C catalyst in comparison to the Pt/C catalyst. The stability of the catalysts was studied in chronoamperometric experiments and the results are presented in Fig. 5. The higher initial current density at 0.2 V on the Pt–Rh–Sn/C catalyst in comparison to the Pt/C catalyst is in accordance with the

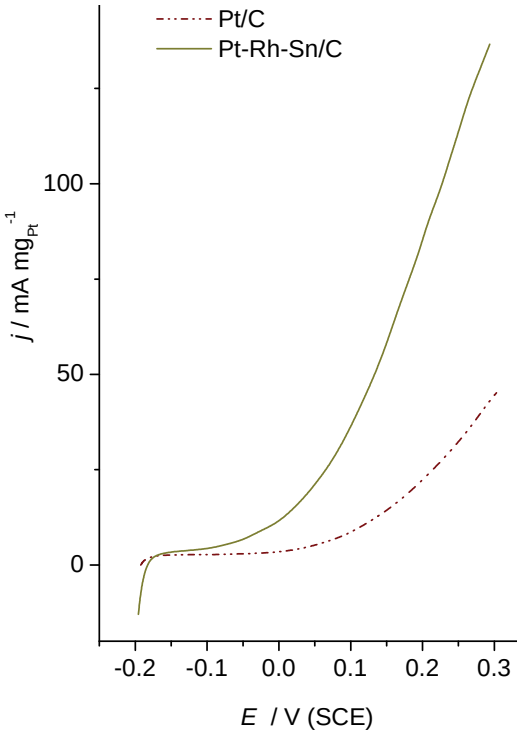

Fig. 4. Potentiodynamic curves for the oxidation of 0.5 M C_2H_5OH at the Pt/C and Pt–Rh–Sn/C catalysts in 0.1 M $HClO_4$, v = 20 mV s^{-1}.

potentiodynamic measurements. The initial current at Pt–Rh–Sn/C stabilizes at a value that was significantly higher than that for the Pt/C catalyst. The Pt–Rh––Sn/C catalyst is evidently more active and less poisoned than the Pt/C catalyst.

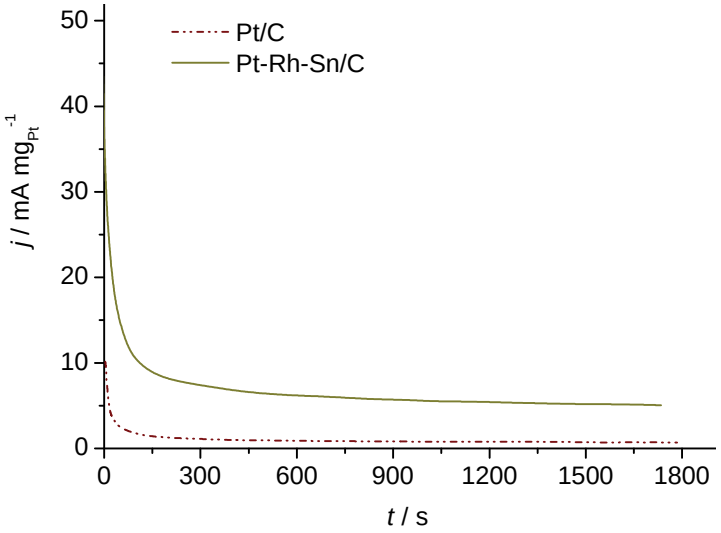

Fig. 5. Chronoamperometric curves for the oxidation of 0.5M C_2H_5OH at 0.2 V at the Pt/C and Pt–Rh–Sn/C catalysts in 0.1 M $HClO_4$.

The better activity for the EOR of the ternary Pt–Rh–Sn catalyst in comparison to Pt/C catalyst must be related to the formation of the ternary alloy. Thus, the presence of Sn and Rh in the catalyst can promote ethanol oxidation by an electronic effect in the Pt-based electrode material affecting the adsorption properties of the surface, making this system less prone to poisoning by organic species than pure Pt. Sn or its oxides can supply surface oxygen-containing species at lower potentials by activation of the interfacial water molecule necessary to complete the oxidation of the adsorbed reaction intermediates leading to carbon dioxide, in the situation that the C−C bond was broken, or to the formation of acetic acid.[12,29] This oxidative removal of CO-like species strongly adsorbed on adjacent Pt active sites proceeds through the so-called bi-functional mechanism. According to density functional theory (DFT) calculations,[14] the role of Rh was to adsorb and stabilize the key intermediate CH_2CH_2O in this route, which leads to the cleavage of C−C bonds. A back donation from the Rh d-band electrons to Pt was proposed. Thus, the presence of Pt could modify the electronic structure of Rh by partially emptying its d-band states enabling its strong bonding to CH_2CH_2O, while the activity of Pt was lowered, thereby preventing the partial oxidation of ethanol on the Pt sites.[14]

In comparison with other Pt–Rh–Sn/C catalysts described in the literature[12–14] in which the atomic fraction of Sn was equal or higher than that of Pt, while the atomic fraction of Rh was much smaller than both Pt and Sn, the presently studied Pt–Rh–Sn/C catalyst with highest fraction of Pt and lowest fraction of Sn exhibited a comparably high activity for ethanol oxidation.

Colmati *et al.*[12] studied ethanol oxidation at Pt–Rh–Sn/C catalysts with molar ratios 1:1:1 and 1:0.3:1, prepared by formic acid oxidation. The ternary catalyst with the lower fraction of Rh was found to have a higher activity, but both the Pt–Rh–Sn/C catalysts exhibited a significantly lower activity in comparison with PtSn/C catalyst at lower potentials (< 0.45 V RHE) and the opposite at higher potential values. The higher activity of PtSn/C was ascribed to the presence of SnO_2 that could supply oxygen-containing species for the oxidative removal of CO and CH_3CO adsorbed on adjacent Pt active sites. The introduction of Rh changes the geometry (Pt−Pt bond distances) and electronic (Pt d-band vacancy) structure of PtSn catalysts, which could improve the adsorption of ethanol and the cleavage of C−C bonds, increasing in this way the activity for ethanol oxidation at higher potentials.[12] For ethanol oxidation, Kowal *et al.*[13] and Li *et al.*[14] used Pt–Rh–SnO_2/C catalysts prepared by the polyol method with conventional heating. XRD Analysis of these catalysts showed the presence of two phases, Pt–Rh alloy and SnO_2. The catalysts were highly active at lower potentials (< 0.5 V RHE). The catalysts were synthesized with different ratios of the components (Pt:Rh:Sn from 3:1:2 to 3:1:6) and the highest activity for ethanol oxidation and capability to split C−C bonds, as revealed by infrared reflection-adsorption spectroscopy (IRRAS), was achieved with Pt–Rh–Sn 3:1:4.[14]

Although XRD analysis of the present catalyst did not give any information except for its very low crystallinity, some reasonable assumptions can be made based on literature data. It can be assumed that, similarly to other Pt–Rh–Sn catalysts, the Pt was alloyed with Rh since, according to the Pt–Rh phase diagram,[29] these two metals form a solid solution at any ratio. XPS and XRD analyses of bimetallic PtSn catalysts prepared by microwave or conventional heating of ethylene glycol solutions of H_2PtCl_6 and $SnCl_2$ salts indicated significant amounts of SnO_2 and rather low degree of alloying.[25,30] Thus, it can be assumed that the Sn in the present Pt–Rh–Sn catalyst existed mainly as SnO_2. Both assumptions mean that the prepared catalyst should be similar to the catalysts obtained by Li *et al.*[14] but with a larger fraction of Rh and a lower fraction of Sn, but still exhibiting a comparable performance. It was shown that the addition of a small quantity of Sn greatly enhanced the electrooxidation of ethanol at low potentials.[28,31] On the other hand, a low amount of Rh added to Pt only slightly improved the CO_2 yield in ethanol oxidation, while the optimum catalyst composition for C−C bond breakage and CO_2 formation was Pt:Rh 1:1 or even better 3:1.[9,10] Hence, the high activity for ethanol oxidation of the present Pt–Rh–Sn/C

catalyst can be explained by a balanced action and well-tuned content of all three components. In addition, the particle size effect cannot be ignored since very small particles of Pt–Rh–Sn/C catalyst contribute to an increase of the active surface area of the catalyst.

CONCLUSIONS

A microwave-assisted polyol method was used to prepare carbon supported Pt and Pt–Rh–Sn nanoparticles with high electrocatalytic activities for the ethanol electrooxidation reaction.

The structural (XRD) and surface characterization (STM) of the catalysts revealed that catalysts with small particles and a rather uniform size distribution were synthesized by this method. This could be attributed to the advantages of the microwave-assisted modified polyol process in ethylene glycol solution.

The electrochemical measurements revealed a high activity of the prepared Pt–Rh–Sn/C catalyst for ethanol oxidation. This catalyst had five times higher oxidation currents and significantly lower reaction onset potential than the Pt/C catalyst. Chronoamperometric measurements confirmed notably less poisoning of the Pt–Rh–Sn/C catalyst than of the Pt/C catalyst. Although with significantly higher fraction of Rh and lower fraction of Sn in comparison to other Pt–Rh–Sn catalysts described in the literature, the catalyst prepared in the present study exhibited a similar shift of onset potential to negative values as well as lower poisoning. The increased activity of Pt–Rh–Sn/C catalyst in comparison to Pt/C catalyst was most probably promoted by the bi-functional mechanism and the electronic effect of the alloyed metals.

Acknowledgements. This work was financially supported by the Ministry of Education and Science of the Republic of Serbia, Contract No. 172060.

И З В О Д

МИКРОТАЛАСНА СИНТЕЗА И КАРАКТЕРИЗАЦИЈА Pt И Pt–Rh–Sn КАТАЛИЗАТОРА ЗА ОКСИДАЦИЈУ ЕТАНОЛА

САЊА СТЕВАНОВИЋ[1], ДУШАН ТРИПКОВИЋ[2], ДЕЈАН ПОЛЕТИ[3], ЈЕЛЕНА РОГАН[3], АМАЛИЈА ТРИПКОВИЋ[1] И ВЛАДИСЛАВА М. ЈОВАНОВИЋ[1]

[1]ИХТМ – Центар за електрохемију, Његошева 12, Београд, [2]Materials Science Division, Argonne National Laboratory, Argonne, IL 60439, USA и [3]Технолошко–металуршки факултет, Универзитет у Београду, Карнегијева 4, Београд

Pt и Pt–Rh–Sn катализатори на угљенику развијене површине су синтетизовани полиол-микроталасним поступком у раствору етиленгликола и испитивани за реакцију елетрохемијске оксидације етанола у киселој средини. Катализатори су окарактерисани структурно, морфолошки и по саставу коришћењем XRD, STM и EDX техника. STM анализа је потврдила да су Pt и Pt–Rh–Sn честице униформне величине и пречника мањег од 2 nm. XRD анализа Pt/C катализатора показала је присуство две фазе, једне са главним карактеристичним пиковима за пљосно-центрирану кубну кристалну структуру платине (111, 200, 220 и 311) и друге са дифракционим пиком на 2θ око 25° карактеристичним за хексагоналну структуру

вулкана XC-72R (угљеничног носача). XRD анализа Pt–Rh–Sn/C катализатора није показала карактеристичне пикове, што је индикација веома мале кристаличности катализатора. Активност катализатора испитивана је потенциодинамичким и хроноамперометријским мерењима. Pt–Rh–Sn/C катализатор је веома активан за оксидацију етанола са почетком реакције на потенцијалима за око 150 mV помереним ка негативнијим вредностима и струјама које су око пет пута веће у поређењу са Pt/C катализатором. Стабилност катализатора испитивана хроноамперометријски показала је да се Pt–Rh–Sn/C катализатор мање troше од Pt/C катализатора. Мала величина и хомогена дистрибуција честица могу се приписати предностима микроталасне синтезе и модификованог полиол поступка у раствору етиленгликола. Већа активност Pt–Rh–Sn/C катализатора у поређењу са Pt/C катализатором последица је би-функционалног механизма и електронског (лиганд) ефекта метала у синтетизованој легури.

(Примљено 5., ревидирано 29. априла 2011)

REFERENCES

1. E. Antolini, *J. Power Sources* **170** (2007) 1
2. A. Lopez-Cudero, J. Solla-Gullon, E. Herrero, A. Aldaz, J. M. Feliu, *J. Electroanal. Chem.* **644** (2010) 117
3. H. Wang, Y. Jusys, R. J. Behm, *J. Power Sources* **154** (2006) 351
4. Q. Wang, G. Q. Sun, L. H. Jiang, Q. Xin, S. G. Sun, Y. X. Jiang, S. P. Chen, Z. Jusys, R. J. Behm, *Phys. Chem. Chem. Phys.* **9** (2007) 2686
5. S. Rousseau, C. Coutanceau, C. Lamy, J. M. Leger, *J. Power Sources* **18** (2006) 158
6. W. Zhou, Z. Zhou, S. Song, W. Li, G. Sun, P. Tsiakaras, Q. Xin, *Appl. Catal., B* 46 (2003) 273
7. W. J. Zhou, S. Q. Song, W. Z. Li, Z. H. Zhou, G. Q. Sun, Q. Xin, S. Douvartzides, P. Tsiakaras, *J. Power Sources* **140** (2005) 50
8. H. Li, G. Sun, L. Cao, L. Jiang, Q. Xin, *Electrochim. Acta* **52** (2007) 6622
9. J. P. I. de Souza, S. L. Queriroz, K. Bergamaski, E. R. Gonzalez, F. C. Nart, *J. Phys. Chem. B* **106** (2002) 9825
10. F. H. Lima, D. Profeti, W. H. Lizcano-Valbuena, E. A. Ticianelli, E. R. Gonzales, *J. Electroanal. Chem.* **617** (2008) 121
11. A. V. Tripković, J. D. Lović, K. Dj. Popović, *J. Serb. Chem. Soc.* **75** (2010) 1559
12. F. Colmati, E. Antolini, E. R. Gonzalez, *J. Alloys Compd.* **456** (2008) 264
13. A. Kowal, S. Lj. Gojković, K. S. Lee, P. Olszewski, Y. E. Sung, *Electrochem. Comm.* **11** (2009) 724
14. M. Li, A. Kowal, K. Sasaki, N. Marinkovic, D. Su, E. Korach, P. Liu, R. R. Adzic, *Electrochim. Acta* **55** (2010) 4331
15. J. Perez, V. A. Paganin, E. Antolini, *J. Electroanal. Chem.* **654** (2011) 108
16. Y. Wang, J. Zhang, X. Wang, J. Ren, B. Zuo, Y. Tang, *Top. Catal.* **35** (2005) 35
17. W. Yu, W. Tu, H. Liu, *Langmuir* **15** (1999) 6
18. W. Kraus, G. Nolze, *PowderCell for Windows*, V.2.4, Federal Institute for Materials Research and Testing, Berlin, Germany, 2000
19. H. P. Klug, L. E. Alexander, *X-Ray diffraction procedures*, 2nd ed., Wiley, New York, 1974, p. 687
20. C. Feldmann, C. Metzmacher. *J. Mater. Chem.* **11** (2001) 2603
21. S. L. Knupp, W. Li, O. Paschos, T. M. Murray, J. Snyder, P. Haldar, *Carbon* **46** (2008) 1276

22. W. X. Tu, H. F. Liu, *Chem. Mater.* **12** (2000) 564
23. S. Song, J. Liu, J. Shi, H. Liu, V. Maragou, Y. Wang, P. Tsiakaras, *Appl. Catal., B* **103** (2011) 223
24. W. Tu, H. Liu, *J. Mater. Chem.* **10** (2000), p. 2207.
25. Z. Liu, B. Guo, L. Hong, T. H. Lim, *Electrochem. Comm.* **8** (2006) 83
26. K. J. Rao, B. Vaidhyanatham, M. Ganguli, P. A. Ramakrishnan, *Chem. Mater.* **11** (1999) 882
27. W. X. Chen, J. Y. Lee, Z. L. Liu, *Chem. Comm.* (2002) 2588
28. F. C. Simoes, D. M. Dos Anjos, F. Vigier, J. M. Leger, F. Hahn, C. Coutanaceau, E. R. Gonyaley, G. Tremiliosi-Filho, A. R. De Andrade, P. Olivi, K. B. Kokoh, *J. Power Sources* **11** (2007) 1567
29. M. Hansen, K. Anderko, *Constitution of binary alloys*, 2nd ed., McGraw-Hill, New York, 1958
30. Z. Liu, L. Hong, S. W. Tay, *Mater. Chem. Phys.* **105** (2007) 222
31. C. Lamy, S. Rousseau, E. M. Belgsir, C. Coutanceau, J. M. Leger, *Electrochim. Acta* **49** (2004) 3901.